Supporting Information

Association with natural organic matter enhances the sunlight-mediated inactivation of MS2 coliphage by singlet oxygen

Tamar Kohn[†*], Matthew Grandbois[§], Kristopher McNeill[§], and Kara L. Nelson [†]

[†]Department of Civil and Environmental Engineering,

Univeristy of California, Berkeley, Berkeley, CA 94720

[§]Department of Chemistry,

76 Kolthoff Hall, University of, Minnesota, Minneapolis, MN, 55455

[*]corresponding author email addess: tamar.kohn@epfl.ch

Pages: 12

Content: Chemicals and Organisms

Total Organic Carbon and Iron analysis

Measurement of $^1O_2$ concentrations with binding plots for the adsorption of the hydrophobic vinyl ether probe to NOM

Correction for light screening

Illustration of NOM-mediated MS2 inactivation

Illustration of some MS2 surface properties

Table of enhancement factors in D_2O and in the presence of Mg^{2+}

Contributions of NOM-associated and bulk phase inactivation to k_{obs}

k_{obs} in (diluted) WSP water

Chemicals and Organisms

Sample solutions contained deionized water, D_2O (99.9%, Aldrich), or water obtained from a waste stabilization pond (WSP) described previously (*1*), NaCl (Fisher), and either phosphate (NaH_2PO_4, Fisher) or bicarbonate ($NaHCO_3$, Fisher) as a buffer. The natural organic matters (NOM) tested were Fluka humic acid (FHA; Fluka), Aldrich Humic Acid (AHA; Aldrich), Suwannee river humic acid (SRHA; International Humic Substance Society) and Pony Lake Fulvic Acid (PLFA; International Humic Substance Society). $MgCl_2$ (Fisher) was added to enhance MS2-NOM interactions. The probe compound for measuring $[^1O_2]_{bulk}$ concentrations was furfuryl alcohol (FFA; 99%, Aldrich). Iron analysis included ferroZine iron reagent (98%, Acros), hydroxylamine hydrochloric reagent (Acros), ammonium acetate (Fisher Chemicals) and sulfuric acid (Fisher Chemicals). Chemiluminecent measurements included tetrabutylammonium fluoride (TBAF 1.0 M in tetrahydrofuran; Aldrich), acetonitrile (ACS grade, Mallinckrodt), and 2-[1-(3-*tert*-butyldimethylsiloxy)phenyl)-1-methoxy-methylene]tricyclo[3.3.1.1]decane (OMe probe, synthesized according to ref. *2*.

MS2 coliphage (ATCC 15597-B1) was cultured and enumerated as described in ref. *3* using the materials listed previously (*1*). Selected MS2 samples were analyzed in triplicate and yielded reproducible results (95% confidence intervals of 0.08 log units). Several MS2 inactivation and $^1O_2$ formation experiments were conducted in duplicate with high reproducibility.

Total organic carbon analysis.

Total organic carbon (TOC) was determined using a Shimadzu TOC-5000 A analyzer.

Measurement of $^1O_2$ concentrations

$[^1O_2]_{bulk}$ during the MS2 inactivation experiments (Oriel solar simulator) was determined by adding a hydrophilic probe compound with a known quenching rate constant, furfuryl alcohol (*4*), to a replicate 150-mL reactor and monitoring its decay. The detection limit for this method was 10^{-15} M.

Measurements of $[^1O_2]_{internal}$ and the ratio $[^1O_2]_{internal}$: $[^1O_2]_{bulk}$ (Atlas solar simulator) were based on the trapping of $^1O_2$ by a vinyl ether probe compound, (2-[1-[(3-tert-butyl-dimethylsilyloxy)phenyl]-1-methoxymethylene]adamantane), (**TPMA**, Figure S1) to form a dioxetane (**TPMA-O_2**, Figure S1). The amount of $^1O_2$ trapped as dioxetane was quantified by inducing the dioxetane to undergo chemiluminescent decomposition. The chemiluminescence intensity was related to the $^1O_2$ concentration by a calibration curve.

Chemiluminescence was recorded via a Turner Designs TD-20/20 Chemiluminometer and analyzed via KaleidaGraph™ (v. 3.5, 2000, Synergy Software) as describe in ref. *5*. Samples (5 mL) contained 5 mM phosphate buffer, 10 mM NaCl, 10 μM of the hydrophobic vinyl ether probe (**TPMA**, Figure S1) for the determination of $[^1O_2]_{internal}$, as well as 100 μM FFA to simultaneously determine $[^1O_2]_{bulk}$. Aliquots of NOM were added to the sample solutions to obtain the NOM concentrations specified. Sampling was executed by taking 100 μL aliquots periodically during photolysis.

The hydrophobic vinyl ether probe partitions between the bulk aqueous environment and hydrophobic environment within NOM to form a complex (**TPMA·NOM**, Figure S1) characterized by its binding coefficient, K_{OM}. Within the complex, **TPMA** reacts with $[^1O_2]_{internal}$ to form **TPMA-O$_2$**. The same intermediate dioxetane is formed when unbound **TPMA** reacts with $[^1O_2]_{bulk}$. Introduction of fluoride initiates chemiluminescence that is recorded and analyzed as the concentration of singlet oxygen apparent to the probe, $[^1O_2]_{app}$, for each irradiation experiment with varied concentration of NOM (Figure S2). These data were fit to Equation S1 (*5*):

$$[^1O_2]_{app} = \frac{K_{OM}[NOM]}{1+K_{OM}[NOM]}\left([^1O_2]_{internal} - [^1O_2]_{bulk}\right) + [^1O_2]_{bulk} \qquad \text{(eq. S1)}$$

Extrapolation of the resulting model fits provided an estimate of $[^1O_2]_{internal}$ for each NOM (Figure S2). Additionally, K_{OM} was determined from the model fits for comparison of hydrophobicity.

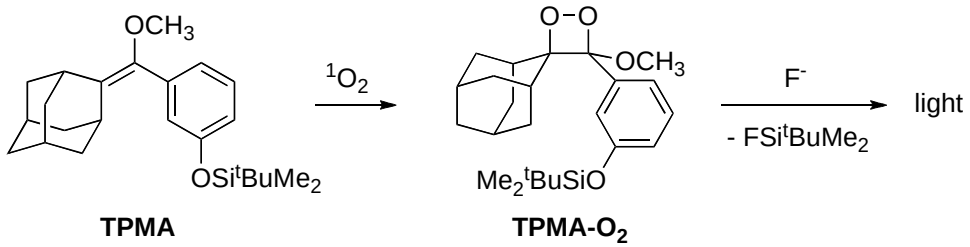

$$\text{TPMA} + \text{NOM} \underset{}{\overset{K_{OM}}{\rightleftharpoons}} \text{TPMA}\cdot\text{NOM} \qquad (1)$$

$$\text{TPMA}\cdot\text{NOM} \xrightarrow{[^1O_2]_{internal}} \text{TPMA-O}_2 \qquad (2)$$

$$\text{TPMA} \xrightarrow{[^1O_2]_{bulk}} \text{TPMA-O}_2 \qquad (3)$$

Figure S1: Reaction of hydrophobic vinyl ether probe (**TMPA**) with singlet oxygen ($^1O_2$) to form **TMPA-O$_2$**. The amount of **TMPA-O$_2$** formed is quantified by subsequent fluoride (F^-) induced chemiluminescent degradation. Equation *1* expresses the equilibrium reached between unbound probe and natural organic matter (NOM) to form the NOM-bound probe (TPMA·NOM). This equilibrium is governed by its binding coefficient, K_{OM}. Dioxetane is formed by reaction of free and bound probe molecules with $[^1O_2]_{bulk}$ and $[^1O_2]_{internal}$, respectively. (Equations *2*-*3*)

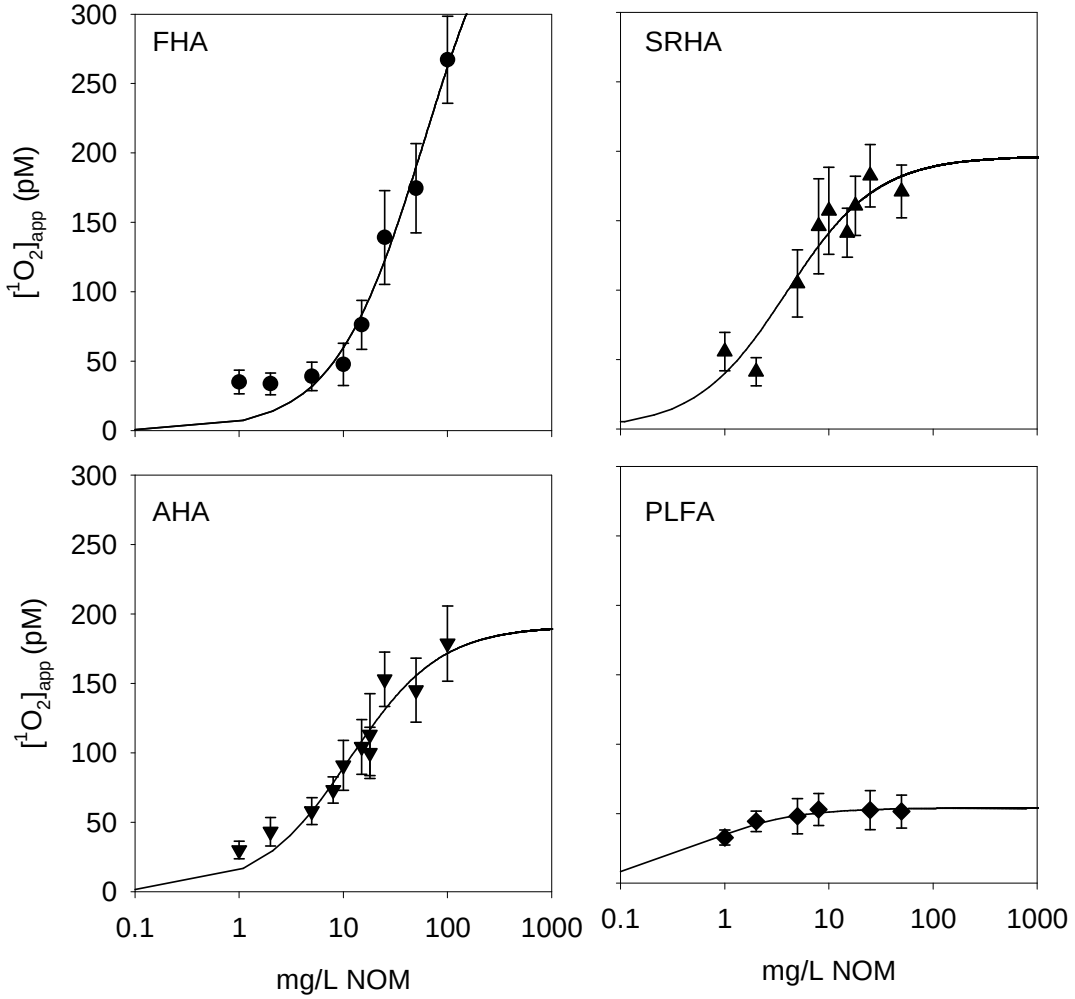

Figure S2: Binding plots for the adsorption of the hydrophobic vinyl ether probe onto NOM. The apparent singlet oxygen concentration, $[^1O_2]_{app}$, reported by the vinyl ether probe was modeled as a weighted sum of the $^1O_2$ concentrations experienced by NOM-bound and -unbound probe molecules (eq. S1; solid line indicates model fits). $[^1O_2]_{internal}$ was determined by extrapolation to the completely bound limit. Error bars indicate 95 % confidence intervals.

Correction for light screening

The light screening correction factor was derived from the comparison of light intensity at the surface of the solution and the mean light intensity over a given solution thickness. At the optically thin surface layer, the rate of light absorption is given by the sum of the light absorbed over the light spectrum (eq. S2).

$$k_{abs,thin} = 2.303\sum_{\lambda}\alpha_{\lambda} I_{\lambda,0} \qquad \text{(eq. S2)}$$

Where α_λ is the light attenuation at a given wavelength and $I_{\lambda,0}$ is the light irradiance at a given wavelength at the surface. Outside the optically thin regime, one must use the mean light intensity, $\langle I_\lambda \rangle_z$, due to the significant absorption within solutions (eq. S3).

$$k_{abs,thick} = 2.303\sum_{\lambda}\alpha_{\lambda}\left\langle I_{\lambda,0}\right\rangle \qquad \text{(eq. S3)}$$

Where the average light irradiance at depth z is the irradiance at the surface multiplied by the light screening factor (eq. S4).

$$\left\langle I_{\lambda}\right\rangle_z = I_{\lambda,0}\frac{(1-10^{-\alpha_\lambda z})}{2.303\alpha_\lambda z} = I_{\lambda,0}S_{\lambda} \qquad \text{(eq. S4)}$$

The correction factor (CF) is then defined as the ratio of light absorbed at optically thin conditions over the light absorbed at optically thick conditions (eq. S5).

$$CF = \frac{k_{abs,thin}}{k_{abs,thick}} = \frac{\sum_{\lambda}\alpha_{\lambda} I_{\lambda,0}}{\sum_{\lambda}\alpha_{\lambda}\left\langle I_{\lambda}\right\rangle_z} = \frac{\sum_{\lambda}\alpha_{\lambda} I_{\lambda,0}}{\sum_{\lambda}\alpha_{\lambda} I_{\lambda,0} S_{\lambda}} \qquad \text{(eq. S5)}$$

The correction factor was applied to data acquired for TPMA and MS2.

Note that this approach does not account for light scattering.

Illustration of NOM-mediated MS2 inactivation

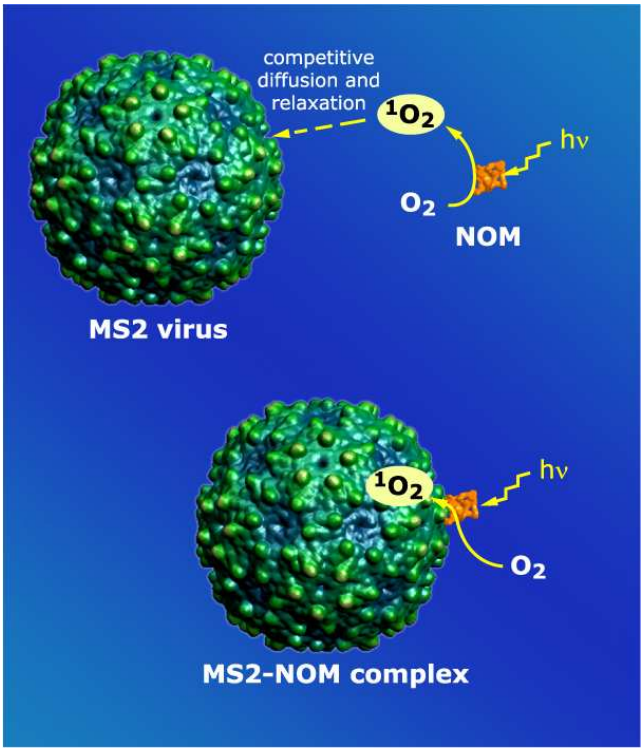

Figure S3: Illustration of NOM-mediated MS2 inactivation in the bulk phase, and by adsorbed NOM. The distance (dotted arrow) between $^1O_2$ and MS2 is greater in the bulk solution than for the MS2-NOM complex, which results in less quenching of $^1O_2$ by the solvent.

Surface heterogeneity of MS2

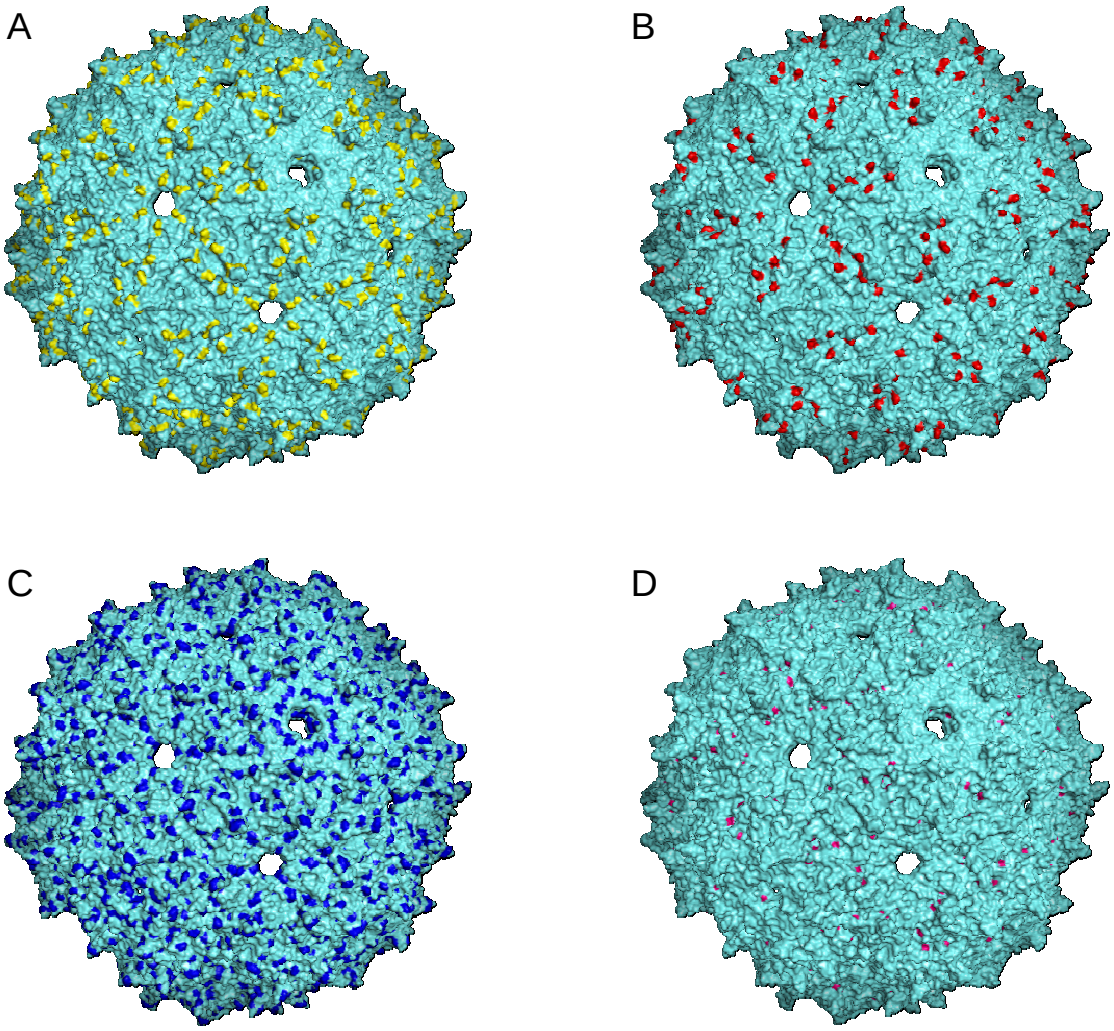

Figure S4: Distribution of acidic, basic, hydrophobic and easily oxidizable groups on the surface of MS2. A: carboxylic acid residues (aspartic acid and glutamic acid); B: basic residues (arginine and lysine; MS2 contains no histidine); C: hydrophobic (aliphatic) residues (glycine, alanine, valine, leucine and isoleucine); D: residues sensitive to oxidation by $^1O_2$ (according to ref. *6*; tyrosine, tryptophane, cysteine and methionine; note that the concentration of $^1O_2$-sensitive residues is higher on the inside surface of MS2). Images were created in pymol, based on pdb file no. 2ms2.

Rate constant enhancement in D_2O and upon addition of Mg^{2+}

Table S1: Enhancement of k_{obs} (at 5 mg/L NOM) in D_2O, and upon addition of 2mM Mg^{2+}. k_{obs} in H_2O and D_2O are corrected for a baseline inactivation (without NOM) of 0.046 h^{-1}. k_{obs} in Mg^{2+} are corrected for a baseline inactivation (without NOM, but with Mg^{2+}) of 0.084 h^{-1}.

	$k_{obs}(D_2O) / k_{obs}(H_2O)$ *(experimental)*	$k_{obs}(D_2O) / k_{obs}(H_2O)$ *(calculated)*[a]	$k_{obs}(Mg^{2+}) / k_{obs}$
FHA	3.0	1.4	2.8
SRHA	5.0	1.4	1.2
AHA	8.1	6.4	3.8
PLFA	10.3	6.5	4.1

[a] Values were calculated based on eq. 5 and the fitting parameters in Table 1, and assuming that $[^1O_2]_{bulk}$ increases 13-fold in D_2O.

Contributions of NOM-associated and bulk phase inactivation to k_{obs}

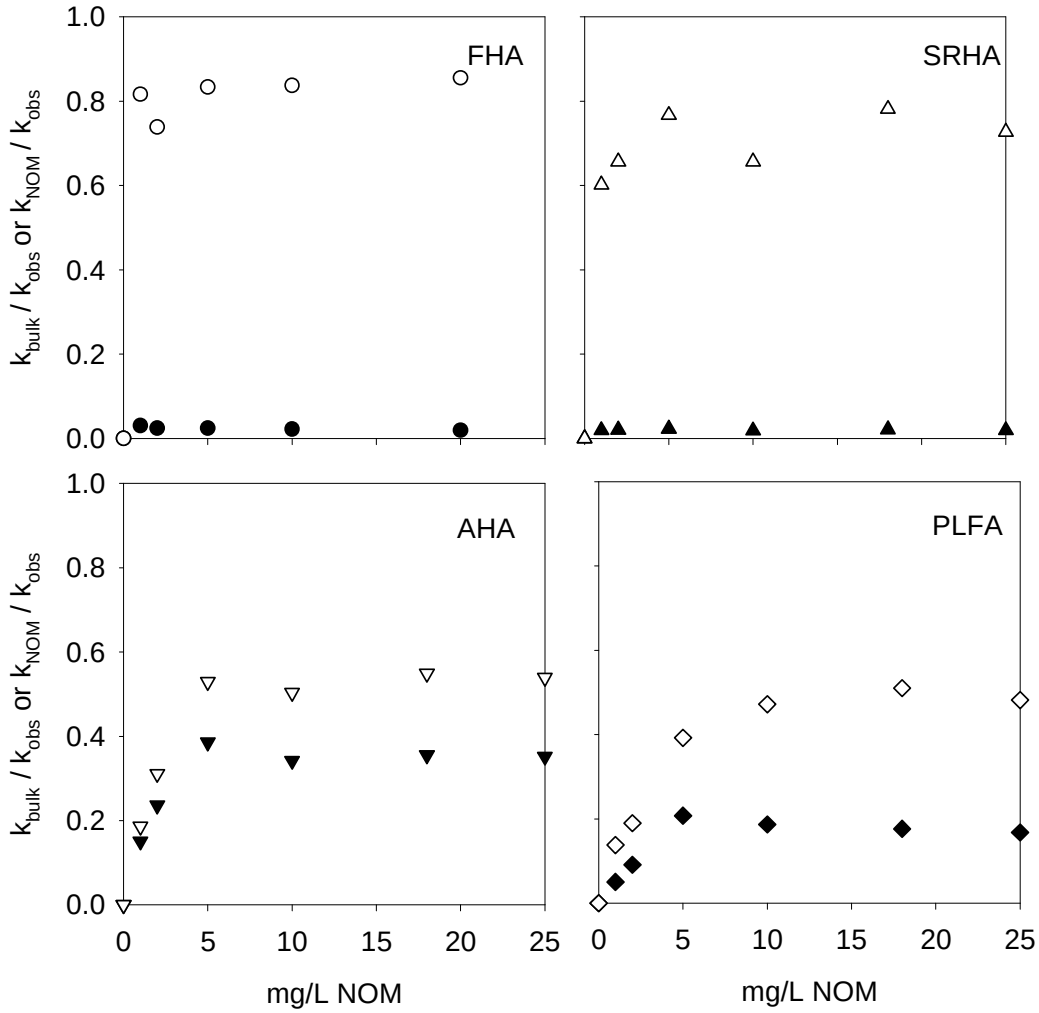

Figure S5: Contributions of NOM-associated (open symbols) and bulk-phase (solid symbols) inactivation to the overall inactivation rate constant k_{obs}. The fractions were calculated as $\frac{k_{NOM} * f_{NOM}}{k_{obs}}$ and $\frac{k_{bulk} * f_{bulk}}{k_{obs}}$, respectively, where k_{obs} is the experimental inactivation rate constant at each NOM concentration. Note that the NOM-associated inactivation is always more dominant than inactivation in the bulk solution.

k_{obs} in (diluted) WSP water

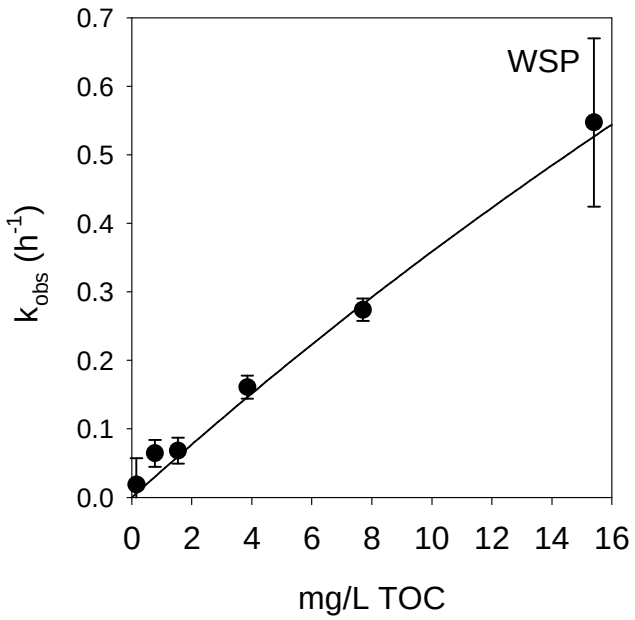

Figure S6: k_{obs} as a function of TOC in (diluted) pond water. The solid line indicates the model fit to equation 5. Error bars indicate 95 % confidence intervals.

Literature cited

1. Kohn, T., and K. L. Nelson**.** Sunlight-mediated inactivation of MS2 coliphage via exogenous singlet oxygen produced by sensitizers in natural waters. *Environ. Sci. Technol.* **2007**. *41,* 192-197.
2. MacManus-Spencer, L. A., D. E. Latch, K. M. Kroncke, and K. McNeill**.** Stable dioxetane precursors as selective trap-and-trigger chemiluminescent probes for singlet oxygen. *Anal. Chem.* **2005**. *77,* 1200-1205.
3. APHA, AWWA, and WEF**.** *Standard Methods for the Examination of Water & Wastewater*; 21 ed. American Public Health Association, American Water Works Association, and Water Environment Federation: Washington, DC, 2005.
4. Haag, W. R., and J. Hoigné**.** Singlet oxgyen in surface waters. 3. Photochemical formation and steady-state concentrations in various types of waters. *Environ. Sci. Technol.* **1986**. *20,* 341-348.
5. Latch, D. E., and K. McNeill**.** Microheterogeneity of singlet oxygen distributions in irradiated humic adic solutions. *Science* **2006**. *311,* 1743-1747.
6. Davies, M. J. Singlet oxygen-mediated damage to proteins and its consequences. *Biochem. Bioph. Res. Co.* **2003**. *305,* 761-770.